Desalination and Water Treatment
www.deswater.com
doi: 10.1080/19443994.2013.852484

52 (2014) 3256–3270
April

Taylor & Francis
Taylor & Francis Group

Removal of Cu^{2+} and Cd^{2+}, and humic acid and phenol by electrocoagulation using iron electrodes

Djamel Ghernaout*, Sara Irki, Ahmed Boucherit

Chemical Engineering Department, University Saad Dahlab of Blida, P.O. Box 270, Blida 09000, Algeria
Tel./Fax: +213 25 43 36 31; email: djamel_andalus@yahoo.fr

Received 2 October 2013; Accepted 3 October 2013

ABSTRACT

This work concerns the plotting current intensity I (A) *vs.* applied voltage E (V) curves of electrocoagulation (EC) of some organic (humic acid (HA) and phenol) and inorganic (copper sulphate and cadmium chloride) compounds which are often found in water/wastewaters. The study is conducted in batch mode using Fe electrodes at laboratory scale. The device is constituted with two ordinary steel electrodes with active area S = 19.95 cm^2 and 4 cm as separation from each other in a 500 mL beaker which is filled with 500 mL solution to treat. The applied voltage is 12 V for 45 min as EC time and an optimal pH which is determined from current intensity I (A) as a function of applied voltage E (V) curves. Depending on the pollutant type, different EC process mechanisms are proposed and less or more important reduction levels are achieved in these experiments.

Keywords: Electrocoagulation (EC); Humic acid (HA); Phenol; Copper; Cadmium; Iron

1. Introduction

In Algeria, the water resources are limited and unevenly distributed. These resources have been, over the last two decades, found to have negative effects like drought and pollution. The absolutely pure water rarely exists in nature. The raw waters still contain many organic and inorganic pollutants from natural or human activity [1]. One of the goals sought in water treatment is to reduce or even eliminate these pollutants [2–4]. This is performed by physicochemical processes (coagulation/flocculation, sedimentation, filtration and disinfection) [5–11]. Currently, there is a tendency to use electrochemical techniques (electrocoagulation (EC), electroflotation, electrooxidation, electrodisinfection, etc.) [12–18] as promising methods for water/wastewater treatment [19–23].

This work aims to contribute in the comprehension of EC process by studying the reduction of some representative pollutants, such as organic (humic acid (HA) and phenol) and inorganic (copper and cadmium) compounds contained in wastewater. Synthetic solutions of these substances are prepared and electrocoagulated at a laboratory scale.

The tests consisted in carrying out electrolysis experiments in an EC reactor. In order to distinguish between the different mechanisms of EC process, first of all, the pH of distilled water is adjusted at three representative values of the pH range: pH 2 (acidic), 7 (neutral) and 12 (alkaline). Then, the solutions are electrolysed as control tests during which the evolution of the current intensity I (A) as a function of the

*Corresponding author.

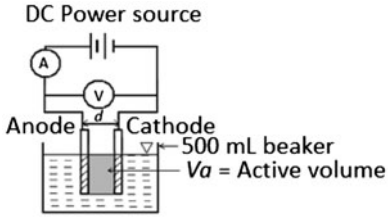

Fig. 1. Diagram of the experimental device with two electrodes (d = 4 cm, distance between electrodes, V_a = Active volume).

applied voltage E (V) is controlled and the phenomena occurring at the cathode, anode and solution are noted. Similarly, the solutions of organic (HA and phenol) and inorganic (copper sulphate and cadmium chloride) compounds are adjusted to the three pH values and then electrolysed. In the end, some EC tests are performed on these solutions.

2. Materials and methods

2.1. Experimental set-up

The EC tests are conducted using an experimental set-up available in the laboratory (Figs. 1 and 2). This installation consists of a glass container (beaker) of 500 mL volume, two ordinary steel electrodes (consisting of 99.8% iron and 0.2% carbon) with 1.9 cm × 20 cm as dimensions and immersed in the reactor. For each electrode, the immersed surface is 19.95 cm^2 (1.9 cm × 10.5 cm)—so the active area A_a (for anode and cathode) is 19.95 cm^2 × 2 = 39.9 cm^2—and the distance between them is fixed at d = 4 cm (these two parameters, i.e. A_a and d, are kept constant throughout this work). The solution volume is 900 mL and the active volume is $V_a = A_a \times d$ = 19.95 × 4 = 79.8 mL

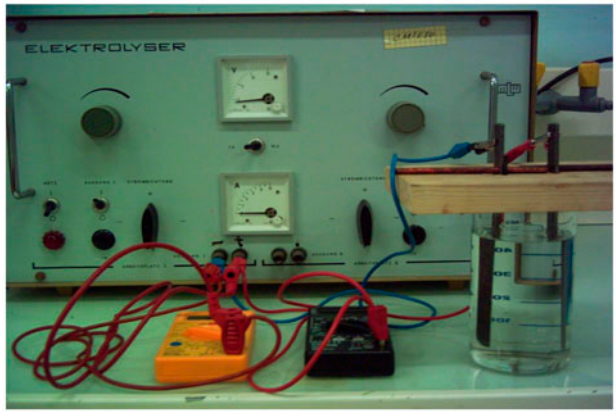

Fig. 2. Photo of the EC experimental set-up.

(Figs. 1 and 2). The concept of the *ratio r active volume (V_a) on reactor volume which is full of water (500 mL)* was introduced in our previous work [24]. The ratio r = 79.8/500 = 0.1596 is suitable for EC process to avoid the dead zones apparition in the reactor. A DC power source ELEKTROLYSER (15 V, 10 A) is connected to the anode and cathode. An ammeter type ALDA DT 89OC and voltmeter type DT 830B DIGITAL to measure the current intensity I (A) and the applied voltage E (V), respectively, are connected to the set-up as shown in Fig. 1. A pH meter type inoLab level 1 is provided for measuring the pH of the solution before and after the electrochemical treatment. A conductivity meter type 250 HANNA instruments is used to measure the conductivity of the solution before and after the EC process. A turbidimeter type WTW—Turb 550 is used to measure the turbidity of the suspension before and after the electrochemical experiment.

2.2. Nature of electrodes

The material of the anode determines the cation introduced into the solution [25]. The most common electrodes are plates of aluminum or iron. However, it should be indicated that the use of iron salts (Fe^{2+}/Fe^{3+}) as a coagulant in water treatment has a significant advantage due to their harmlessness compared to aluminum salts (Al^{3+}) that have some toxic effects [25]. On the other hand, the relatively higher efficiency of iron electrodes may be attributed to the size of the cation produced which is 10–30 μm for Fe^{3+} compared to the 0.05–1 μm for Al^{3+} [26].

2.3. Electrodes cleaning

Before any test, the electrodes are prepared to avoid the presence of any impurity as follows: (1) polishing with abrasive paper; (2) rinsing with distilled water; (3) degreasing by means of a solution composed of: NaOH (25 g), Na_2CO_3 (25 g), K_2CO_3 (25 g) and distilled water (q.s.p. 1,000 mL); (4) rinsing with distilled water; (5) pickling in a solution of sulphuric acid (H_2SO_4) at 20% for 20 min at room temperature; and again (6) rinsing with distilled water.

2.4. Prepared solutions

The solutions used are prepared with analytical grade products: (1) HA (ACROS Humic acid, Sodium salt, tech); (2) phenol (C_6H_5OH, M = 94.11 g mol^{-1}, at 99.5%, Chiminova Internacional 28,016 Madrid—Spain); (3) copper sulphate ($CuSO_4$ $5H_2O$,

M = 249.68 g mol^{-1}, at 98.5%, Laboratory NTL, Nentech LTD); and (4) cadmium chloride ($CdCl_2.2.5H_2O$, M = 227.4 g mol^{-1}, at 99.5%, Laboratory NTL, Nentech LTD).

A concentrated solution at 1 g L^{-1} is prepared by dissolving 1 g of HA in 62.5 mL of NaOH (2 N) solution in 1 L phial and then completed to 1 L with distilled water. This solution is submitted to magnetic agitation during 48 h and then conserved at 4˚C in the absence of light. From this solution, diluted solutions (10 mg L^{-1}) are prepared for EC tests.

2.5. Analytical techniques

2.5.1. UV–vis spectrophotometry

For the organic compounds, HA and phenol, UV–vis spectrometry is used to quantify the organic solutions. The principle of this method is based on the absorption of monochromatic radiation by a given solution in the UV–vis spectrum. For HA and phenol, the UV absorbances are experimentally determined at the wavelengths λ = 254 and 270 nm, respectively. The analysis method is based on the use of the calibration curve Abs = f (c) following the Beer–Lambert formula. Determining an unknown concentration c_x corresponding to an absorbance Abs is determined graphically by extrapolation. All solutions are analysed by a spectrophotometer type VARIAN CARY 50 Scan.

From the concentrated solution of HA 1 g L^{-1}, solutions at different concentrations are prepared in vials of 100 mL. The solutions pH is adjusted at 12 using a solution of 2 N NaOH and the corresponding absorbances are measured at 254 nm. Without adjusting pH, the same procedure is applied for phenol at 270 nm. In Figs. 3 and 4, the calibration curves for HA and phenol are shown. As seen in Figs. 3 and 4, good correlations are achieved for both HA and phenol curves showing the exactitude of the UV–vis spectrophotometery method.

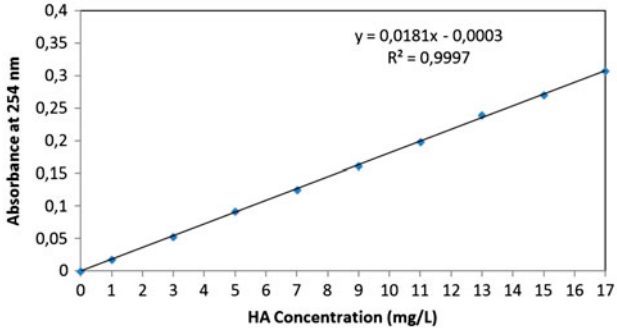

Fig. 3. Calibration curve for HA concentration as a function of absorbance at 254 nm at pH 12.

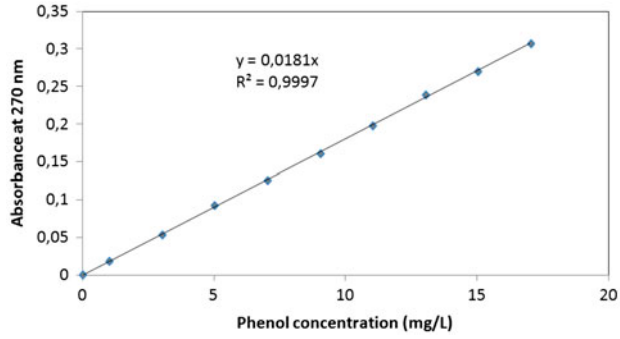

Fig. 4. Calibration curve for phenol: phenol concentration *vs.* absorbance at 270 nm.

2.5.2. Atomic absorption spectrophotometry

In order to control the concentration of metallic elements during the process of EC, atomic absorption spectrophotometry is used. For our metal analysis, an apparatus type AAS Pye Unicam SP9 (Philips) is used.

2.6. Methods

In order to study the EC process and understand its involved mechanisms and reactions, several experiments are made. First of all, I = f (E) scanning curves are performed with distilled water as control before organic (HA and phenol) and inorganic compounds (copper sulphate and cadmium chloride). Then, HA, phenol, copper sulphate and cadmium chloride are taken separately where scanning curves are performed. Finally, EC treatment experiments are realised for each pollutant.

3. Results and discussion

3.1. Current intensity vs. applied voltage scanning curves for distilled water

Control solutions of distilled water at different pH (acidic, neutral and alkaline) are electrolysed without agitation and subjected to 30 min of sedimentation before filtration on a Buchner funnel. The filtrates are allowed to stand for analyses. For each pH, the applied voltage E is swept from 0 to 15 V and maintained constant during 2 min for each value. Current intensity *vs.* applied voltage scanning curves for distilled at different pH are presented in Fig. 5. As seen in Fig. 5, the electric current passes best in the EC reactor when pH is acidic and then at alkaline pH and finally at neutral pH. For pH 7, the current intensity values are relatively very low as the maximum value is 11.54 mA, so their curve is near the x-axis (Fig. 5).

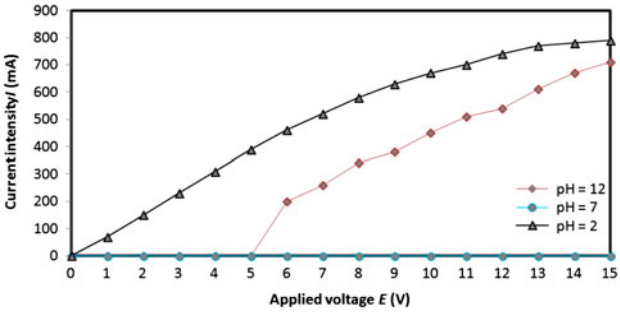

Fig. 5. Current intensity I (mA) *vs.* applied voltage E (V) for distilled water at different pH values.

For pH 12, the six first-values are so low (their maximum value is at 141.9 mA) that they are near the x-axis and the following points start to increase so they are distinguished from the x-axis (Fig. 5). For pH 2, the first-value for 1 V is 50 mA so the acidic curve is more distinguished from the two other curves.

3.1.1. Acidic pH

At pH 2 and for E = 1 V, there is a weak release of hydrogen bubbles at the cathode on both sides (anode and container). For E = 4 V, there is a low release of oxygen bubbles on the anode (cathode side). For E = 7 V, there is a vigorous evolution of hydrogen. For E = 10 V, the cathode at the anode side begins to darken. For E = 12 V, there is decomposition of the black deposit on the cathode which was previously formed to produce green-black flocs. At the end of the experiment, the deposit of iron oxide that was previously attached to the cathode settles down to the bottom. The vigorous evolution of H_2 bubbles at the cathode and the low evolution of O_2 at the anode [27,28] and the appearance of green-black flocs, $Fe(OH)_{2(S)}$ according to Murugananthan et al. [29], are due to the following reactions:

Anode:

$$2Fe_{(S)} - 4e^- \rightarrow 2Fe^{2+}_{(aq)} \quad (1)$$

$$2H_2O_{(1)} - 4e^- \rightarrow O_{2(g)} + 4H^+_{(aq)} \quad (2)$$

Solution:

$$2Fe^{2+}_{(aq)} + 4OH^-_{(aq)} \rightarrow 2Fe(OH)_{2(S)} \quad (3)$$

Total:

$$2Fe_{(S)} + 6H_2O_{(1)} \rightarrow O_{2(g)} + 4H_{2(g)} + 2Fe(OH)_{2(S)} \quad (4)$$

Reaction (4) takes into account the observed production of oxygen at the anode and hydrogen at the cathode and of the appearance of green-black $Fe(OH)_{2(S)}$ flocs in the solution. For the cathode at the side of the anode which begin to blacken: it is the ferrous oxide which is depositing on the cathode [27].

3.1.2. Neutral pH

At pH 7 and for E = 7 V, there is low H_2 bubbling on the cathode at the anode side and the appearance of green colour in the solution. For E = 15 V, a cloud of brown colloids get out of the anode to the cathode. The observed green colour indicates the presence of ferrous ions, Fe^{2+} and/or bihypoferrites, $HFeO_2^-$. The brown-red colour which occurred is due to the presence of solid ferric hydroxide, $Fe(OH)_{3(S)}$ and/or hematite, Fe_2O_3 [27]. For Kovacheva-Ninova [28], the brown to yellow-orange colour indicates $Fe(OH)_{3(S)}$ presence. The following reactions are possible for this pH:

Anode:

$$2Fe_{(S)} - 4e^- \rightarrow 2Fe^{2+}_{(aq)} \quad (5)$$

$$2Fe^{2+}_{(aq)} - e^- \rightarrow Fe^{3+}_{(aq)} \quad (6)$$

$$Fe_{(S)} - 3e^- \rightarrow Fe^{3+}_{(aq)} \quad (7)$$

Solution:

$$Fe^{2+}_{(aq)} + 2OH^-_{(aq)} \rightarrow 2Fe(OH)_{2(S)} \quad (8)$$

$$2Fe^{3+}_{(aq)} + 6OH^-_{(aq)} \rightarrow 2Fe(OH)_{3(S)} \quad (9)$$

Cathode:

$$8H_2O_{(1)} + 8e^- \rightarrow 4H_{2(g)} + 8OH^-_{(aq)} \quad (10)$$

Total:

$$3Fe_{(S)} + 8H_2O_{(1)} \rightarrow 2Fe(OH)_{2(S)} + 2Fe(OH)_{3(S)} + 4H_{2(g)} \quad (11)$$

Reaction (9) takes into account the appearance of green colloids, $Fe(OH)_{2(S)}$, in solution and then red-brown colloids, $Fe(OH)_{3(S)}$, and H_2 production

Table 1
Initial and final conditions of the scan at different pH for distilled water

	Parameter	Initial state	Final state
Acidic pH	pH	2	2.62
	Turbidity (NTU)	2.1	3.1
	Conductivity (μS cm^{-1})	9450.0	2910.0
	Cathode mass (g)	91.36	91.36
	Anode mass (g)	91.68	91.68
Neutral pH	pH	7	6.59
	Turbidity (NTU)	2.1	3.6
	Conductivity (μS cm^{-1})	47.5	12.5
	Cathode mass (g)	91.37	91.37
	Anode mass (g)	91.71	91.70
Alkaline pH	pH	12	12.07
	Turbidity (NTU)	3.6	4.3
	Conductivity (μS cm^{-1})	5,880	5,880
	Cathode mass (g)	91.34	91.34
	Anode mass (g)	91.39	91.37

from the cathode. For the conversion of ferrous ions to ferric ions, Murugananthan et al. [29] proposed the term auto-oxidation, and Kovacheva-Ninova [28] referred to a series of reactions from metallic iron to ferric iron at the anode:

$$Fe_{(S)} \xrightarrow{H_2O} Fe(OH)_{ads} \xrightarrow{H_2O,O_2} Fe(OH)_{2(S)} + Fe^{2+}.nH_2O \xrightarrow{H_2O,O_2} Fe(OH)_{3(S)}$$

3.1.3. Alkaline pH

At pH 12 and for E = 2 V, there is strong H_2 bubbling (cathode) and low O_2 release (anode). For E = 7 V, there is appearance of a cloud of brown-yellowish colloids at the anode (cathode side) and agglomeration of flocs. The presence of a brown colour in the solution is due to the presence of ferric ions. The ferric ions, in the intense presence of $OH^-_{(aq)}$, give rise to ferric hydroxide, $Fe(OH)_{3(S)}$, according to the following reactions:

Anode:

$$2Fe_{(S)} - 6e^- \rightarrow 2Fe^{3+}_{(aq)} \quad (13)$$

Solution:

$$2Fe^{3+}_{(aq)} + 6OH^-_{(aq)} \rightarrow 2Fe(OH)_{3(S)} \quad (14)$$

Cathode:

$$6H_2O_{(1)} + 6e^- \rightarrow 3H_{2(g)} + 6OH^-_{(aq)} \quad (15)$$

Total:

$$2Fe_{(S)} + 6H_2O_{(1)} \rightarrow 2Fe(OH)_{3(S)} + 3H_{2(g)} \quad (16)$$

Reaction (11) reflects the appearance red-brown colloids, $Fe(OH)_{3(S)}$, in solution and the H_2 production at the cathode. The initial and final conditions of the scan at different pH values for distilled water are shown in Table 1. At the end of the scan I = f (E) for all pH for distilled water, the cathode mass did not change regardless of the pH value. However, the anode mass slightly decreased as follows: for acidic pH, the mass reduction is 0.294%; at neutral pH, it is 0.01%; and at alkaline pH, it is 0.021%.

3.2. Electrocoagulation of organic compounds

3.2.1. Humic acid solution

3.2.1.1. Current intensity vs. applied voltage scanning curves for humic acid. Similar tests as done with distilled water are performed with 15 mg L^{-1} HA solution. Fig. 6 presents I = f(E) scanning curves for HA at different pH values and Table 2 summarises the initial and final conditions of these experiments. As seen in Fig. 6, the electric current flows better in the acidic medium, and then in the alkaline medium, and finally in the neutral environment. The curves behaviour in Fig. 6 for HA is similar to the curves behaviour in Fig. 5 for distilled water. However, the acidic curve is more distinguished from x-axis as in Fig. 5 for distilled water.

3.2.1.1.1. Remarks

(a) *Acidic pH*: For pH 2 and E = 1 V, there is low H_2 (cathode) and O_2 (anode) bubbling. For E = 4 V, the anode begin to blacken (at the cathode inside) and the H_2 bubbling become intense. For E = 7 V, there is appearance of a foam at the solution surface near the cathode. For E = 9 V, there is formation of a green deposit on the cathode surface from the bottom to the top.

(b) *Neutral pH*: For pH 7 and E = 5 V, there is a low release of H_2 (cathode). For E = 11 V, there is appearance of a brown cloud of colloids emerging from the anode surface and sediment at the bottom of the container. For E = 15 V, there is appearance of a new cloud still green at the anode.

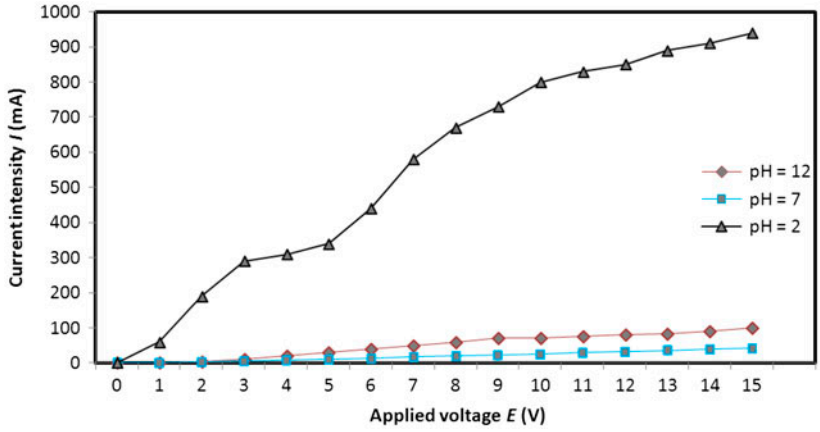

Fig. 6. Current intensity I (mA) *vs.* applied voltage E (V) for 15 mg L^{-1} HA solution at different pH values.

Table 2
Initial and final conditions of the scan at different pH for 15 mg L^{-1} HA solution

	Parameter	Initial state	state
Acidic pH	pH	2	1.63
	Turbidity (NTU)	5.2	2.6 (50%)
	Conductivity (μS cm^{-1})	5,170	1,230
	Cathode mass (g)	90.44	90.44
	Anode mass (g)	88.90	88.51
	Absorbance (254 nm)	0.346	0.00807 (97.67%)*
Neutral pH	pH	7	5.7
	Turbidity (NTU)	4	0.63 (84.25%)*
	Conductivity (μS cm^{-1})	234	224
	Cathode mass (g)	90.19	90.19
	Anode mass (g)	88.19	88.18
	Absorbance (254 nm)	0.346	0.5746 (−66.06%)*
Alkaline pH	pH	12	12.7
	Turbidity (NTU)	4	13 (−225%)*
	Conductivity (μS cm^{-1})	1,050	1,190
	Cathode mass (g)	90.28	90.28
	Anode mass (g)	88.34	88.31
	Absorbance (254 nm)	0.346	0.5759 (−66.44%)*

*Results between brackets present the reduction efficiencies.

(c) *Alkaline pH*: For pH 12 and E = 3 V, there is release of H_2 (cathode) and O_2 (anode). For E = 5 V, there is formation of a brown deposit on the anode (at the cathode side and then at the reactor side). For E = 8 V, a green deposit appears on the anode. For E = 12 V, there is a green-and-brown-cloudiness release.

3.2.1.1.2. Interpretations

(a) *Acidic pH:* The change of green to black colour indicates the presence of Fe^{2+} ions in the solution. The decrease in turbidity (50%) and absorbance (97.67%) (see Table 2) are due to the formation of a metal humic complex. In the surface complexation mode, HA being a negatively charged organic molecule which acts as a ligand (L) to chemically bond with the hydrated iron according to the following reactions [25]:

$$L^-_{(aq)} + H^+_{(aq)}) \rightarrow LH_{(aq)} \quad (17)$$

$$LH_{(aq)} + (OH)OFe_{(aq)} \rightarrow LH(OH)OFe_{(aq)} \quad (18)$$

$$LH(OH)OFe_{(aq)} \rightarrow LOFe_{(S)} + H_2O_{(1)} \quad (19)$$

(b) *Neutral and alkaline pH:* The green colour indicates the presence of Fe^{2+} ions and the brown colour indicates the presence of Fe^{3+} ions. The increase in turbidity is due to the formation of metal hydroxides appearing in the solution:

$$L^-_{(aq)} + OH^-_{(aq)} \rightarrow L(OH)^{2-}_{(aq)} \quad (20)$$

The increase in absorbance (66.06% in neutral pH and 66.44% in alkaline pH) indicates the phenomenon of re-stabilisation. Indeed, initially, negatively charged macromolecules see their solubility increase in a neutral or basic pH. In addition, the macromolecules are split into smaller molecules by the action of Fe $(OH)_4{}^-{}_{(aq)}$, $Fe(OH)_2{}^{2-}{}_{(aq)}$, etc.

3.2.1.2. Removal tests of humic acid solution. The HA solutions at different concentrations (5, 10 and 20 mg L^{-1}) are electrolysed for a treatment time of 45 min and an applied voltage set at 12 V (the maximum applied voltage allowed by the power supply is 15 V) at pH = 2. The initial and final conditions of these tests are carried in Table 3. In these experimental conditions, i.e. stabilised voltage, we have observed a vigorous H_2 and O_2 bubbling, a green deposit on the cathode and appearance of brown flocs in the solution. Reactions (4) and (10) explain the above observations. As seen in Table 3, the HA removal increases from 45.44 to 92.47 and 94.67%, when HA concentration increase from 5 to 10 and 20 mg L^{-1}, respectively. Consequently, the HA removal is relatively proportional to the HA concentration.

Feng et al. [30] and Vepsäläinen et al. [31] indicated that the EC reaction performance is dependent on initial pH value, i.e. the lower pH values lead to faster reactions and better efficiency. It is well established that pH of the solution directly influence the HA configuration. Indeed, an aromatic ring is the basic element of HA which may be considered as a reticular macromolecule polymer connected by hydrogen bonds between functional retentions. The most active functional retentions are carboxyl and phenolic hydroxyl groups, and the dissociation of H^+ relates to pH value of solution. In other words, when pH is acidic, carboxyl and hydroxyl groups exist in the chemical form of –COOH and –OH, respectively. However, if pH is alkaline, they exist in the form of $–COO^-$ and $–O^-$. Obviously, under conditions of a higher pH, HA takes on a more negative charge and more Fe^{2+}/Fe^{3+} is consumed to neutralise the humic negative charge. Consequently, the treatment efficiency will decrease under higher pH values [30,32].

Labanowski et al. [33] concluded that EC increased the amount of hydrophilic organic compounds of lower apparent molecular weight. However, their remark needs more research to better understand the electrochemical transformation of organic matter. For Vepsäläinen et al. [34], the mechanism of NOM removal by EC was similar to chemical coagulation in different pH values. Moreover in low pH, double-layer compression was the main destabilisation mechanism whereas in higher pH, adsorption and bridging dominated [33,34].

Table 3
Initial and final conditions of the HA treatment at different concentrations at pH 2

Concentration (mg L^{-1})	Parameter	Initial state	Final state
5	pH	2	1.59
	Conductivity (μS cm^{-1})	1,050	2,870
	Turbidity (NTU)	1.28	0.08 (93.75%)
	Anode mass (g)	88.77	88.73
	Cathode mass (g)	89.62	89.62
	Absorbance (254 nm)	0.114	0.0622 (45.44%)
10	pH	2	2.04
	Conductivity (μS cm^{-1})	740	1,800
	Turbidity (NTU)	2.15	0.97 (54.88%)
	Anode mass (g)	84.87	84.43
	Cathode mass (g)	87.84	87.84
	Absorbance (254 nm)	0.231	0.0174 (92.47%)
20	pH	2	3.50
	Conductivity (μS cm^{-1})	900	1,300
	Turbidity (NTU)	3.02	0.59 (80.46%)
	Anode mass (g)	91.16	90.84
	Cathode mass (g)	91.25	91.25
	Absorbance (254 nm)	0.46	0.0245 (94.67%)

3.2.2. Phenol solution

3.2.2.1. Current intensity vs. applied voltage scanning curves for phenol. Similar to those made earlier, some tests are conducted for phenol solutions at 15 mg L^{-1}. Fig. 7 presents $I = f(E)$ curves for 15 mg L^{-1} phenol solutions at different pH. Table 4 presents the initial and final conditions of scanning curves experiments for 15 mg L^{-1} phenol solutions. As seen in Table 4 and Fig. 7, the electric current flows best in the solution that has a high conductivity (following this order alkaline, acidic and finally neutral medium), i.e. in alkaline pH. In comparison between Figs. 6 (HA) and 7 (phenol), the curves order is inversed for Fig. 7: alkaline curve > acidic curve > neutral curve. These curves tendencies (Figs. 6 and 7) prove that the phenol molecule is more conductive of the electric current in alkaline pH at the same time the HA molecule is more conductive of electric current in acidic medium. Consequently, the pH value has a great role in organic molecule configuration and solution behaviour in electrochemical process.

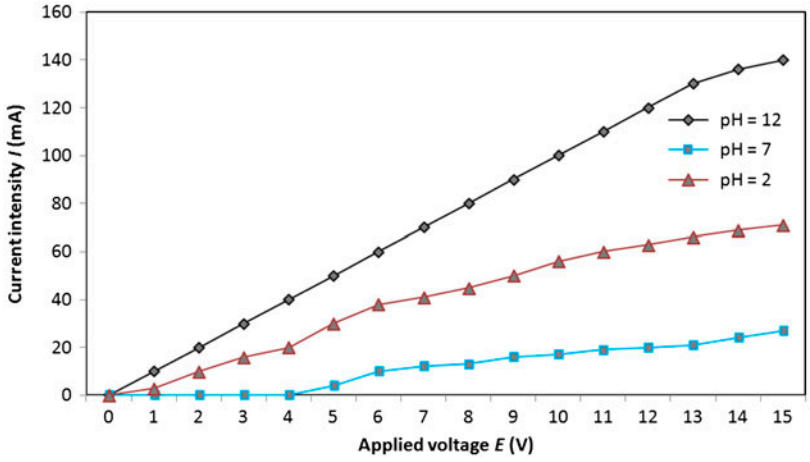

Fig. 7. Current intensity I (mA) *vs.* applied voltage E (V) for 15 mg L^{-1} phenol solution at different pH values.

3.2.2.1.1. Remarks

(a) *Acidic pH*: For pH = 2 and E = 3 V, there is start of H_2 bubbling on the cathode. For E = 11 V, the cathode begins to blacken.

(b) *Neutral pH*: For pH 7 and E = 5 V, there is a low H_2 bubbling on the cathode. For E = 8 V, there is appearance of a brown cloud of colloids on the anode. For E = 12 V, a cloud of green colloids appears on the anode.

(c) *Alkaline pH*: For pH 12 and E = 4 V, there is H_2 bubbling at the cathode and O_2 bubbling at the anode. For E = 6 V, there is formation of a brown deposit on the anode. For E = 8 V, there is emergence of a new green deposit at the bottom of the anode. The O_2 bubbles transport the flocs formed on the anode to the surface.

3.2.2.2. Interpretations. (a) *Acidic pH*: Conductivity, turbidity and absorbance (270 nm) decreased. These decreases may be due to the phenol removal under the Fe^{2+} action following Reaction (16):

$$2Ar-OH_{(aq)} + Fe^{2+}_{(aq)} \rightarrow (Ar-O)_2Fe_{(s)} + 2H^{+}_{(aq)} \quad (21)$$

(b) *Neutral pH*: The absorbance of the neutralised solution increased from 0.270 to 0.367 and so the conductivity and turbidity (Table 4). This can be explained by the formation of a new species or a mixture proportions according to the Reaction (17):

$$Ar-OH_{(aq)} + NaOH_{(aq)} \leftrightarrow Ar-ONa_{(aq)} + H_2O_{(l)} \quad (22)$$

(c) *Alkaline pH*: At pH 12, parameters, such as conductivity, turbidity and absorbance (270 nm) are reduced due to the phenol removal following these reactions:

$$Ar-OH_{(aq)} + NaOH_{(aq)} \leftrightarrow Ar-ONa_{(aq)} + H_2O_{(l)} \quad (23)$$

$$2Ar-ONa_{(aq)} + Fe^{2+}_{(aq)} \rightarrow (Ar-O)_2Fe_{(s)} + 2Na^{+}_{(aq)} \quad (24)$$

$$3Ar-ONa_{(aq)} + Fe^{3+}_{(aq)} \rightarrow (Ar-O)_3Fe_{(s)} + 3Na^{+}_{(aq)} \quad (25)$$

Table 4
Initial and final conditions of 15 mg L^{-1} phenol solution scanning at different pH values

	Parameter	Initial state	Final state
Acidic pH	pH	2	2.58
	Turbidity (NTU)	0.18	0.02 (88.88%)
	Conductivity (μS cm^{-1})	700	300
	Cathode mass (g)	91.06	91.06
	Anode mass (g)	90.61	90.61
Neutral pH	Absorbance (270 nm)	0.270	0.205 (24.07%)
	pH	7	6.40
	Turbidity (NTU)	0.2	3.63 (−1,715%)
	Conductivity (μS cm^{-1})	70	89.1
	Cathode mass (g)	89.76	89.76
	Anode mass (g)	87.45	87.39
Alkaline pH	Absorbance (270 nm)	0.270	0.367 (−35.92%)
	pH	12	11.84
	Turbidity (NTU)	2.3	1.03 (55.22%)
	Conductivity (μS cm^{-1})	1,170	760
	Cathode mass (g)	89.89	89.89
	Anode mass (g)	89.80	89.77
	Absorbance (270 nm)	0.270	0.261 (3.33%)

Following Table 4, absorbance (270 nm) is relatively well reduced at pH 2.

3.2.2.3. Removal tests of phenol solution. Phenolic solutions at different concentrations (5, 10 and 20 mg L^{-1}) are electrolysed for a treatment time of 45 min and an applied voltage set to 12 V. Table 5 presents the initial and final conditions of these experiments. In these experiments, where the applied voltage is set at 12 V during 45 min, a vigorous H_2 bubbling on the cathode, a green deposit on the cathode and appearance of brown flocs in the solution are observed. Several authors [35–37] achieved similar results.

Table 5
Initial and final conditions of 15 mg L^{-1} phenol solution electrolysed at pH 2 during 45 min at 12 V

Concentration (mg L^{-1})	Parameter	Initial state	Final state
5	pH	2	3.49
	Conductivity (μS cm^{-1})	898	140
	Turbidity (NTU)	0.13	0.03 (76.92%)
	Anode mass (g)	88.43	88.41
	Cathode mass (g)	73.70	73.70
	Absorbance (270 nm)	0.092	0.085 (7.61%)
10	pH	2	3.51
	Conductivity (μS cm^{-1})	906	150
	Turbidity (NTU)	0.15	0.05 (66.67%)
	Anode mass (g)	85.69	85.65
	Cathode mass (g)	88.51	88.51
	Absorbance (270 nm)	0.185	0.15 (18.92%)
20	pH	2	4.04
	Conductivity (μS cm^{-1})	965	127
	Turbidity (NTU)	0.18	0.05 (72.22%)
	Anode mass (g)	85.61	85.57
	Cathode mass (g)	80.06	80.06
	Absorbance (270 nm)	0.262	0.153 (41.60%)

3.3. Electrocoagulation of inorganic compounds

3.3.1. Copper sulphate solution

3.3.1.1. Scanning curves of copper sulphate solution. Scanning tests, similar to those made previously, are performed for copper sulphate solutions of 15 mg L^{-1} concentration of the copper element. Fig. 8 presents $I = f(E)$ scanning curves for copper solution. Table 6 presents the initial and final conditions of 15 mg L^{-1} copper solution scanning at different pH values. Fig. 8 shows that the electric current flows better in the alkaline, acidic and neutral medium.

3.3.1.1.1. Remarks

(a) *Acidic pH*: For pH 2 and E = 2 V, there is H_2 bubbling on the cathode. For E = 10 V, there is formation of a black deposit on the cathode (in small amounts) which is followed by the appearance of some brown flocs on the cathode and on the surface of the solution.

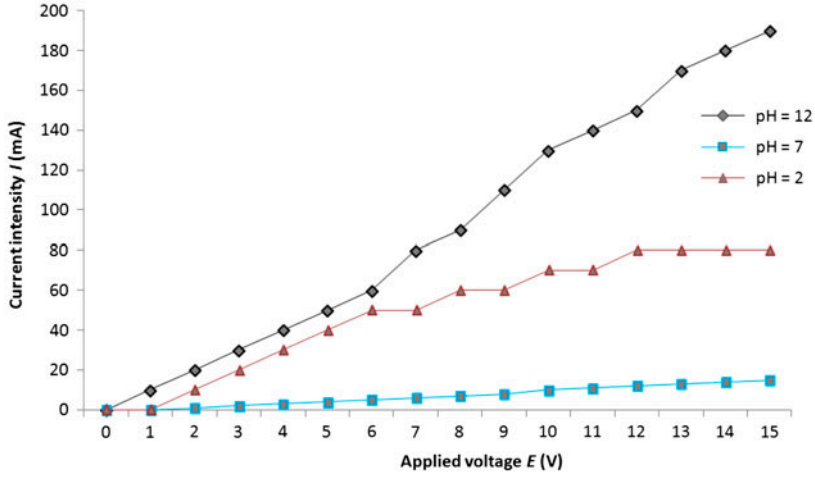

Fig. 8. Current intensity I (mA) *vs.* applied voltage E (V) for 15 mg L^{-1} copper solution at different pH values.

Table 6
Initial and final conditions of 15 mg L^{-1} copper solution scanning at different pH values

	Parameter	Initial state	Final state
Acidic pH	pH	2	2.08
	Turbidity (NTU)	0.36	0.10 (72.22%)
	Conductivity (μS cm^{-1})	1,060	852
	Cathode mass (g)	88.08	88.08
	Anode mass (g)	85.16	85.13
	Concentration (mg L^{-1})	15	13.20 (12%)
Neutral pH	pH	7	4.28
	Turbidity (NTU)	3.20	1.66 (48.12%)
	Conductivity (μS cm^{-1})	76.60	190
	Cathode mass (g)	88.52	88.52
	Anode mass (g)	85.80	85.79
	Concentration (mg L^{-1})	15	0.45 (97%)
Alkaline pH	pH	12	11.66
	Turbidity (NTU)	4.22	0.27 (93.60%)
	Conductivity (μS cm^{-1})	1,410	1,000
	Cathode mass (g)	88.47	88.47
	Anode mass (g)	85.72	85.69
	Concentration (mg L^{-1})	15	0.19 (98.73%)

(b) *Neutral pH*: Once sodium hydroxide (NaOH) is added to obtain a neutral pH, the solution becomes cloudy (blue) and this is due to the formation of Cu $(OH)_{2(s)}$ precipitates. For E = 8 V, there is appearance of a cloud of brown colloids around the anode. For E = 11 V, there is a low H_2 bubbling on the cathode.

(c) *Alkaline pH*: There is always the formation of a blue precipitate, $Cu(OH)_{2(s)}$, when sodium hydroxide (NaOH) is added to increase pH to 12. For E = 2 V, there is H_2 bubbling at the cathode and O_2 bubbling at the anode and formation of a green deposit on the anode. For E = 8 V, there is formation of another brown deposit still on the anode. For E = 10 V, there is decomposition of the deposits and release of some flocs in the solution.

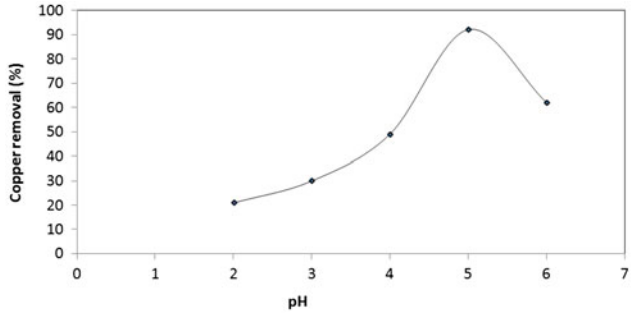

Fig. 9. Copper EC removal efficiencies as a function of the solution pH.

3.3.1.1.2. Interpretations

(a) *Acidic pH*: The turbidity and conductivity decreases are due to the formation of $Cu(OH)_{2(s)}$ which reduce copper concentration from the solution. This reduction is due to the combination of Cu^{2+} and OH^- ions which are generated by the water electrolysis to give $Cu(OH)_{2(s)}$.

(b) *Neutral and alkaline pH*: The decrease in conductivity and turbidity is due to the large formation of Cu $(OH)_{2(s)}$ following the NaOH addition to adjust pH to 7 and 12. In order to confirm the fact that the NaOH addition is responsible for the copper removal, the final concentrations of copper solutions were measured after adding NaOH to pH 7 and 12 without EC after 1 h of settling. Table 7 presents the initial and final copper concentrations of solutions after adding NaOH to adjust pH to 7 and 12 without any EC treatment.

3.3.1.2. Electrocoagulation of copper sulphate solution

3.3.1.2.1. Effect of pH

In order to determine the optimum pH of EC treatment, some tests for copper solutions are made at a concentration of 15 mg L^{-1} and at different pH values. The applied voltage E and EC time are, respectively, 12 V and 45 min. Fig. 9 presents copper removal at

Table 7
Initial and final copper concentrations of solutions after adding NaOH to adjust pH to 7 and 12 without EC

	pH 7			pH 12		
Initial concentration (mg L^{-1})	15	20	50	15	20	50
Final concentration (mg L^{-1})	0.49 (96.73%)	0.89 (95.55%)	3.69 (92.62%)	0.26 (98.27%)	0.35 (98.25%)	0.68 (98.64%)

Table 8
Initial and final conditions of copper solutions EC treatment at different concentrations at E = 12 V for 45 min

Concentration (mg L^{-1})	Parameter	Initial state	Final state
3	pH	5	7.09
	Conductivity (μS cm^{-1})	21.6	40
	Turbidity (NTU)	0.33	0.15 (54.54%)
	Anode mass (g)	83.77	83.38
	Cathode mass (g)	72.78	72.78
	Concentration (mg L^{-1})	3	1.23 (59%)
5	pH	5	6.74
	Conductivity (μS cm^{-1})	30	39
	Turbidity (NTU)	0.39	0.17 (56.41%)
	Anode mass (g)	80.50	80.49
	Cathode mass (g)	78.56	78.56
	Concentration (mg L^{-1})	5	1.5 (70%)
10	pH	5	6.79
	Conductivity (μS cm^{-1})	59	33
	Turbidity (NTU)	0.52	0.12 (76.92%)
	Anode mass (g)	80.45	80.44
	Cathode mass (g)	78.52	78.52
	Concentration (mg L^{-1})	10	1.2 (88%)

different pH values. According to Fig. 9, the optimum pH is 5.

Akbal and Camcı [38] achieved total removal of Cu^{2+} at pH 3 using Fe–Al electrode pairs. Mouedhen et al. [39] achieved 98% removal using supporting electrolyte. Hanay and Hasar [40] reached almost 100% after 5 min at pH values > 7. Tsouris et al. [41] removed copper at pH 10 and 12. Fu and Wang [42] reviewed removal of heavy metal ions from wastewaters using particularly EC method. For Escobar et al. [43], the copper removal reached a maximum value of 80%. For Huang et al. [44], a 10-min treatment removed more than 99.5% of the cadmium. Emamjomeh and Sivakumar [45] reviewed metal removal by EC method.

3.3.1.2.2. Effect of copper concentration

Copper solutions at different concentrations (3, 5 and 10 mg L^{-1}) are electrolysed, for a treatment time of 45 min and an applied voltage set to 12 V. Table 8 summarises the initial and final conditions of these experiments. As seen in Table 8, copper removal increases from 59, 70, to 88%, when copper concentration increase from 3, 5, to 10 mg L^{-1}, respectively.

These results show that the copper removal efficiency is relatively proportional to its concentration. For these tests, low H_2 bubbling at the cathode, cloud of brown colloids leaving the anode to the solution and the solution turning brown are observed.

3.3.2. Cadmium chloride solution

3.3.2.1. Scanning curves of cadmium chloride solution. Scanning tests, similar to those made previously, are performed for solutions of cadmium chloride at 15 mg L^{-1} concentration of the cadmium element. The evolution of I = f (E) is shown in Fig. 10. Fig. 10 shows that the electric current flows better in the alkaline, acidic and then neutral medium. Table 9 shows the initial and final conditions of electrolysed Cd^{2+} solutions.

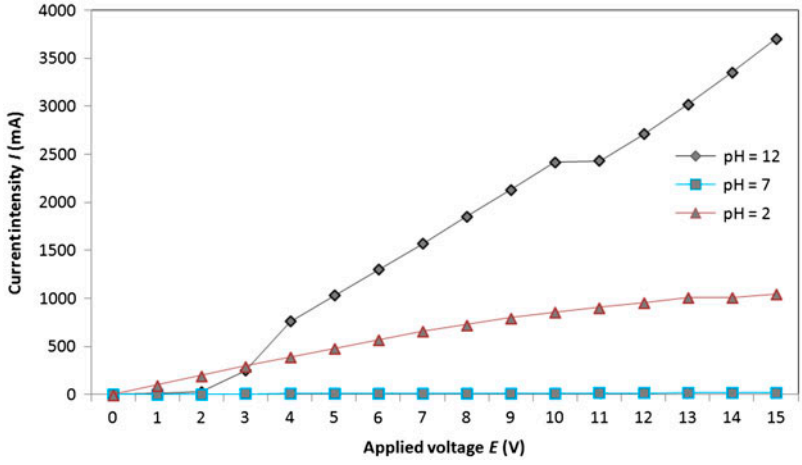

Fig. 10. Scan of the current intensity I (mA) as a function of the applied voltage E (V) to the cadmium solution (15 mg L^{-1}).

Table 9
Initial and final conditions of scanning at different pH for the 15 mg L^{-1} cadmium solution

	Parameter	Initial state	Final state
Acidic pH	pH	2	2.5
	Turbidity (NTU)	0.35	0.31 (11.43%)
	Conductivity (μS cm^{-1})	8,900	3,900
	Anode mass (g)	81.6	81.6
	Cathode mass (g)	79.21	78.86
	Concentration (mg L^{-1})	15	8.40 (44%)
Neutral pH	pH	7	7.23
	Turbidity (NTU)	0.5	0.31 (38%)
	Conductivity (μS cm^{-1})	47	543
	Anode mass (g)	79.28	79.28
	Cathode mass (g)	81.68	81.67
	Concentration (mg L^{-1})	15	5.2 (65.33%)
Alkaline pH	pH	12	11.1
	Turbidity (NTU)	3	0.34 (88.67%)
	Conductivity (μS cm^{-1})	23,500	7,025
	Anode mass (g)	78.85	78.85
	Cathode mass (g)	81.84	81.57
	Concentration (mg L^{-1})	15	0.26 (98.27%)

3.3.2.1.1. Remarks

(a) *Acidic pH*: For pH 2 and E = 1 V, there is a strong H_2 bubbling on the cathode and low O_2 emission from the anode. For E = 7 V, the cathode begins to blacken. For E = 9 V, there is formation of a black deposit at the bottom of the cathode. For E = 12 V, there is decomposition of the deposit.

(b) *Neutral pH*: For pH 7 and E = 7 V, there is a low H_2 bubbling at the cathode. For E = 8 V, there is occurrence of a brown colour in the container bottom. For E = 9 V, the solution becomes brown and there is appearance of a white foam on the solution surface around the cathode.

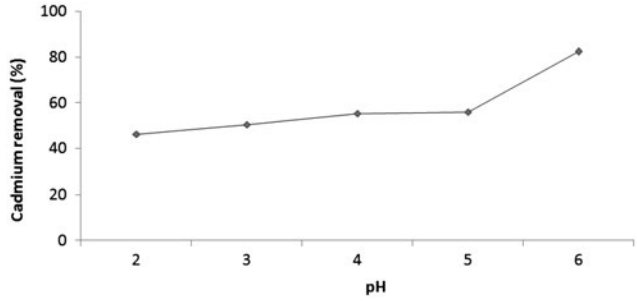

Fig. 11. Cadmium removal efficiencies as a function of the solution pH.

(c) *Alkaline pH*: For pH 12, there is formation of a white precipitate [$Cd(OH)_{2(s)}$] at pH 12 adjustment. For E = 2 V, there is H_2 bubbling at the cathode and O_2 (and/or Cl_2) bubbling on the anode.

3.3.2.1.2. Interpretations

(a) *Acidic pH*: The decrease in conductivity indicates that the removal of Cd^{2+} is by precipitation of the hydroxide, $Cd(OH)_{2(s)}$.

(b) *Neutral and alkaline pH*: The high reduction of conductivity and cadmium concentration is due to the formation of $Cd(OH)_{2(s)}$ during the NaOH addition. Similar to those made previously for copper, some tests are done to confirm that the addition of NaOH is responsible for the removal of cadmium. The results obtained are shown in Table 10.

3.3.2.2. Electrocoagulation tests of cadmium chloride solution.

3.3.2.2.1. Effect of pH

For the determination of the pH effect on EC treatment of cadmium solution, some tests are carried out at a concentration of 15 mg L^{-1} and different pH values. The same conditions (applied voltage and EC time) previously achieved in copper solutions are applied for cadmium solutions. Fig. 11 shows the evolution of Cd efficiency removal as a function of pH. Fig. 11 shows that the efficiency removal increase when pH increase from 2 to 6.

3.3.2.2.2. Effect of concentration

Cadmium solutions were electrolysed at different concentrations (3, 5 and 10 mg L^{-1}) under the same conditions (applied voltage and EC time) applied

Table 10
Initial and final cadmium concentrations of solutions after adding NaOH to adjust pH to 7 and 12 without EC

	pH 7			pH 12		
Initial concentration (mg L^{-1})	15	20	50	15	20	50
Final concentration (mg L^{-1})	7.52 (49.87%)	10.43 (47.85%)	14.30 (71.40%)	0.54 (96.40%)	0.83 (95.85%)	1.20 (97.60%)

Table 11
Initial and final conditions of different EC treatment concentrations

Concentration (mg L^{-1})	Parameter	Initial state	Final state
	pH	6	6.96
	Conductivity (S cm^{-1})	15.3	23
3	Turbidity (NTU)	0.2	0.19 (5%)
	Anode mass (g)	80.56	80.55
	Cathode mass (g)	78.59	78.59
	Concentration (mg L^{-1})	3	1.32 (56%)
	pH	6	8.18
	Conductivity (S cm^{-1})	22	25
5	Turbidity (NTU)	0.22	0.22 (0%)
	Anode mass (g)	83.35	83.34
	Cathode mass (g)	72.75	72.75
	Concentration (mg L^{-1})	5	1.85 (63%)
	pH	6	7.26
	Conductivity (S cm^{-1})	24	38
10	Turbidity (NTU)	0.3	0.25 (16.67%)
	Anode mass (g)	83.29	83.28
	Cathode mass (g)	72.72	72.72
	Concentration (mg L^{-1})	10	1.76 (82.4%)

previously. Table 11 shows the initial and final characteristics of these tests. For these tests, there is a low H_2 bubbling at the cathode; there is also a cloud of brown colloids out of the anode, and the solution turns brown were observed. EC efficiency increases as cadmium concentration increase: 56, 63 and 82.4% for 3, 5 and 10 mg L^{-1}, respectively (Table 11). From these results, it may be concluded that the cadmium reduction efficiency is relatively proportional to the concentration.

Escobar et al. [43] optimised Cu, Pb and Cd removal in natural waters and simulated wastewater and achieved good results as those obtained in our work. Vasudevan and Lakshmi [46] obtained 98% removal of cadmium. Similar performance was reached by Kobya et al. [47] and Orescanin et al. [48].

4. Conclusions

In this work, the I (A) = f(E (V)) scanning curves reveal some interesting organic and inorganic compounds behaviours in EC process. At a less important degree, we have studied at a laboratory scale in batch mode the feasibility of reduction of some organic and inorganic pollutants by EC process. Several removal yields were achieved:

- For HA, the obtained removals are the following: 46, 92.5 and 95.25 for these concentrations: 5, 10 and 20 mg L^{-1}, respectively.
- For phenol, the obtained removals are the following: 7.6, 18.9 and 41.6 for these concentrations: 5, 10 and 20 mg L^{-1}, respectively.
- For copper, the obtained removals are the following: 59, 70 and 88% for these concentrations: 3, 5 and 10 mg L^{-1}, respectively.
- For cadmium, the obtained removals are the following: 56, 63 and 82.4% for these concentrations: 3, 5 and 10 mg L^{-1}, respectively.

By examining the results obtained in this study, we found that the removal efficiency is relatively proportional to the concentration of the pollutant. This suggests that it is sufficient that a fraction of pollutant molecules being electrochemically neutralised by the metal ion to form a nucleus or seed of flocculation on which other no neutralised molecules will be adsorbed. This is what we call here the "snowball effect", to finally produce flocs.

Moreover, HA is better reduced than phenol, and copper more than cadmium. Therefore, the EC process remains a promising process of water/wastewater treatment. It would be desirable to continue this work in continuous mode and for solutions composed with several compounds. Finally, the I (A) = f(E (V)) scanning curves must be performed before the removal of pollutants in EC process in order to more understand the related phenomena.

References

[1] J.T. Alexander, F.I. Hai, T.M. Al-aboud, Chemical coagulation-based processes for trace organic contaminant removal: Current state and future potential, J. Environ. Manage. 111 (2012) 195–207.
[2] D. Ghernaout, B. Ghernaout, M.W. Naceur, Embodying the chemical water treatment in the green chemistry—A review, Desalination 271 (2011) 1–10.
[3] D. Ghernaout, M.W. Naceur, A. Aouabed, On the dependence of chlorine by products generated species formation of the electrode material and applied charge during electrochemical water treatment, Desalination 270 (2011) 9–22.
[4] D. Ghernaout, M.W. Naceur, B. Ghernaout, A review of electrocoagulation as a promising coagulation process for improved organic and inorganic matters removal by electrophoresis and electroflotation, Desalin. Water Treat. 28 (2011) 287–320.
[5] D. Ghernaout, B. Ghernaout, A. Kellil, Natural organic matter removal and enhanced coagulation as a link

between coagulation and electrocoagulation, Desalin. Water Treat. 2 (2009) 203–222.
[6] A. Matilainen, M. Vepsäläinen, M. Sillanpää, Natural organic matter removal by coagulation during drinking water treatment: A review, Adv. Colloid Interface 159 (2010) 189–197.
[7] B. Ghernaout, D. Ghernaout, A. Saiba, Algae and cyanotoxins removal by coagulation/flocculation: A review, Desalin. Water Treat. 20 (2010) 133–143.
[8] D. Ghernaout, B. Ghernaout, From chemical disinfection to electrodisinfection: The obligatory itinerary? Desalin. Water Treat. 16 (2010) 156–175.
[9] D. Ghernaout, B. Ghernaout, On the controversial effect of sodium sulphate as supporting electrolyte on electrocoagulation process: A review, Desalin. Water Treat. 27 (2011) 243–254.
[10] D. Ghernaout, B. Ghernaout, Sweep flocculation as a second form of charge neutralisation—A review, Desalin. Water Treat. 44 (2012) 15–28.
[11] D. Ghernaout, B. Ghernaout, On the concept of the future drinking water treatment plant: Algae harvesting from the algal biomass for biodiesel production—a review, Desalin. Water Treat. 49 (2012) 1–18.
[12] D. Ghernaout, B. Ghernaout, A. Boucherit, M.W. Naceur, A. Khelifa, A. Kellil, Study on mechanism of electrocoagulation with iron electrodes in idealised conditions and electrocoagulation of humic acids solution in batch using aluminium electrodes, Desalin. Water Treat. 8 (2009) 91–99.
[13] D. Ghernaout, B. Ghernaout, A. Saiba, A. Boucherit, A. Kellil, Removal of humic acids by continuous electromagnetic treatment followed by electrocoagulation in batch using aluminium electrodes, Desalination 239 (2009) 295–308.
[14] Y. Yavuz, A.S. Koparal, Ü.B. Öğütveren, Treatment of petroleum refinery wastewater by electrochemical methods, Desalination 258 (2010) 201–205.
[15] D. Ghernaout, M.W. Naceur, Ferrate(VI): *In situ* generation and water treatment—A review, Desalin. Water Treat. 30 (2011) 319–332.
[16] S. Cotillas, J. Llanos, P. Cañizares, S. Mateo, M.A. Rodrigo, Optimization of an integrated electrodisinfection/electrocoagulation process with Al bipolar electrodes for urban wastewater reclamation, Water Res. 47 (2013) 1741–1750.
[17] E. Lacasa, E. Tsolaki, Z. Sbokou, M.A. Rodrigo, D. Mantzavinos, E. Diamadopoulos, Electrochemical disinfection of simulated ballast water on conductive diamond electrodes, Chem. Eng. J. 223 (2013) 516–523.
[18] A.K. Lee, D.M. Lewis, P.J. Ashman, Harvesting of marine microalgae by electroflocculation: The energetics, plant design, and economics, Appl. Energy 108 (2013) 45–53.
[19] D. Ghernaout, A. Badis, A. Kellil, B. Ghernaout, Application of electrocoagulation in *Escherichia coli* culture and two surface waters, Desalination 219 (2008) 118–125.
[20] D. Ghernaout, A. Mariche, B. Ghernaout, A. Kellil, Electromagnetic treatment doubled electrocoagulation of humic acid in continuous mode using response surface method for its optimisation and application on two surface waters, Desalin. Water Treat. 22 (2010) 311–329.
[21] A. Saiba, S. Kourdali, B. Ghernaout, D. Ghernaout, In *Desalination* to 2009, the birth of a new seawater pretreatment process: Electrocoagulation–an overview, Desalin. Water Treat. 16 (2010) (1987) 201–217.
[22] M. Ahmadi, H. Amiri, S.S. Martínez, Treatment of phenol-formaldehyde resin manufacturing wastewater by the electrocoagulation process, Desalin. Water Treat. 39 (2012) 176–181.
[23] D.S. Filho, G.B. Bota, R.B. Borri, F.J.C. Teran, Electrocoagulation/flotation followed by fluidized bed anaerobic reactor applied to tannery effluent treatment, Desalin. Water Treat. 37 (2012) 359–363.
[24] D. Belhout, D. Ghernaout, S. Djezzar-Douakh, A. Kellil, Electrocoagulation of a raw water of Ghrib Dam (Algeria) in batch using aluminium and iron electrodes, Desalin. Water Treat. 16 (2010) 1–9.
[25] M.Y.A. Mollah, R. Schennach, J.R. Parga, D.L. Cocke, Electrocoagulation (EC)—science and applications, J. Hazard. Mater. B84 (2001) 29–41.
[26] P. Holt, G. Barton, C. Mitchell, Electrocoagulation as a wastewater treatment. The Third Annual Australian Environmental Engineering Research Event. Castlemaine, Australia, November 23–26 1999.
[27] M. Pourbaix, Atlas d'équilibres électrochimiques. Verlag Gauthier-Villars, Paris, 1963.
[28] V. Kovacheva-Ninova, Electrochemical treatment of mine waste waters containing heavy metal ions, Annual, vol. 46, part II, Mining and Mineral Processing, Sofia, 2003, pp. 215–220.
[29] M. Murugananthan, G.B. Raju, S. Prabhakar, Removal of sulfide, sulfate and sulfite ions by electro coagulation, J. Hazard. Mater. B109 (2004) 37–44.
[30] Q. Feng, X. Li, Y. Cheng, L. Meng, Q. Meng, Removal of humic acid from groundwater by electrocoagulation, J. China Univ. Min. Technol. 17 (2007) 513–515.
[31] M. Vepsäläinen, M. Ghiasvand, J. Selin, J. Pienimaa, E. Repo, M. Pulliainen, M. Sillanpää, Investigations of the effects of temperature and initial sample pH on natural organic matter (NOM) removal with electrocoagulation using response surface method (RSM), Sep. Purif. Technol. 69 (2009) 255–261.
[32] M. Kobya, E. Gengec, Decolourization of melanoidins by a electrocoagulation process using aluminium electrodes, Environ. Technol. 33 (2012) 2429–2438.
[33] J. Labanowski, V. Pallier, G. Feuillade-Cathalifaud, Study of organic matter during coagulation and electrocoagulation processes: Application to a stabilized landfill leachate, J. Hazard. Mater. 179 (2010) 166–172.
[34] M. Vepsäläinen, M. Pulliainen, M. Sillanpää, Effect of electrochemical cell structure on natural organic matter (NOM) removal from surface water through electrocoagulation (EC), Sep. Purif. Technol. 99 (2012) 20–27.
[35] O. Abdelwahab, N.K. Amin, E.-S.Z. El-Ashtoukhy, Electrochemical removal of phenol from oil refinery wastewater, J. Hazard. Mater. 163 (2009) 711–716.
[36] R. Katal, H. Pahlavanzadeh, Influence of different combinations of aluminum and iron electrode on electrocoagulation efficiency: Application to the treatment of paper mill wastewater, Desalination 265 (2011) 199–205.
[37] M. Uğurlu, A. Gürses, Ç. Doğar, M. Yalçın, The removal of lignin and phenol from paper mill effluents by electrocoagulation, J. Environ. Manage. 8 (2008) 420–428.
[38] F. Akbal, S. Camcı, Copper, chromium and nickel removal from metal plating wastewater by electrocoagulation, Desalination 269 (2011) 214–222.

[39] G. Mouedhen, M. Feki, M. De Petris Wery, H.F. Ayedi, Behavior of aluminum electrodes in electrocoagulation process, J. Hazard. Mater. 150 (2008) 124–135.
[40] Ö. Hanay, H. Hasar, Effect of anions on removing Cu^{2+}, Mn^{2+} and Zn^{2+} in electrocoagulation process using aluminum electrodes, J. Hazard. Mater. 189 (2011) 572–576.
[41] C. Tsouris, D.W. DePaoli, J.T. Shor, M.Z.-C. Hu, R.-Y. Ying, Electrocoagulation for magnetic seeding of colloidal particles, Colloid Surf. A 177 (2001) 223–233.
[42] F. Fu, Q. Wang, Removal of heavy metal ions from wastewaters: A review, J. Environ. Manage. 92 (2011) 407–418.
[43] C. Escobar, C. Soto-Salazar, M.I. Toral, Optimization of the electrocoagulation process for the removal of copper, lead and cadmium in natural waters and simulated wastewater, J. Environ. Manage. 81 (2006) 384–391.
[44] C.-H. Huang, L. Chen, C.-L. Yang, Effect of anions on electrochemical coagulation for cadmium removal, Sep. Purif. Technol. 65 (2009) 137–146.
[45] M.M. Emamjomeh, M. Sivakumar, Review of pollutants removed by electrocoagulation and electrocoagulation/flotation processes, J. Environ. Manage. 90 (2009) 1663–1679.
[46] S. Vasudevan, J. Lakshmi, Effects of alternating and direct current in electrocoagulation process on the removal of cadmium from water—A novel approach, Sep. Purif. Technol. 80 (2011) 643–651.
[47] M. Kobya, E. Demirbas, N.U. Parlak, S. Yigit, Treatment of cadmium and nickel electroplating rinse water by electrocoagulation, Environ. Technol. 31 (2010) 1471–1481.
[48] V. Orescanin, R. Kollar, K. Nad, The electrocoagulation/advanced oxidation treatment of the groundwater used for human consumption, J. Environ. Sci. Health., Part A 46 (2011) 1611–1618.